AIAA SciTech Forum
11–15 & 19–21 January 2021, VIRTUAL EVENT
AIAA Scitech 2021 Forum

10.2514/6.2021-1745

Wall temperature effect on hypersonic turbulent boundary layers via DNS

Guillermo Araya*, Christian Lagares†, Jean Santiago‡ and Kenneth Jansen §

*, †, ‡ HPC and Visualization Lab, Dept. of Mechanical Eng., U. of Puerto Rico at Mayagüez, PR 00681, USA

§ Dept. of Aerospace Eng. Sciences, University of Colorado at Boulder, CO 80309, USA

Direct simulation of hypersonic spatially-developing turbulent boundary layers (SDTBL) was carried out over Zero-Pressure Gradient (ZPG) flat plates at a Mach number of 5 and at different wall thermal conditions: wall cooling, adiabatic and wall heating. The Reynolds number range ($Re_{\delta 2}$) is approximately 300-1200, based on the momentum thickness, freestream velocity and wall viscosity. Turbulent inflow information is generated via a dynamic rescaling-recycling approach (J. Fluid Mech., 670, pp. 581-605, 2011), which avoids the use of empirical correlations in the computation of inlet turbulent scales and it has been adapted to hypersonic flow. In addition, low/high order flow statistics are compared with DNS of an incompressible isothermal ZPG boundary layer at similar low Reynolds numbers and the temperature regarded as a passive scalar. It was concluded that wall normal transport of Reynolds shear stresses significantly increased as the wall temperature increases in the hypersonic regime. Furthermore, large thermal turbulent structures look more organized (anisotropy increase) with more intense "gaps" of freestream fluids in between as wall cooling is applied. The thermal structures appear less organized but more isotropic as the wall temperature is increased.

Nomenclature

C_f	Skin friction coefficient
δ	Boundary layer thickness at 99% U_∞
M_∞	Freestream Mach number
P_r	Molecular Prandtl number
R_{δ_2}	Momentum thickness Reynolds number
T_∞	Freestream temperature
T_r	Recovery temperature
T_w	Wall temperature
U_∞	Freestream velocity
U^+_{VD}	Van Driest transform velocity in wall units
ν_w	Wall kinematic viscosity
u_τ	Friction velocity
Superscript	
$+$	Wall-Units
$'$	Fluctuations
Subscript	
inl	inlet
rec	recycle
$_{rms}$	Root-Mean Squared

*Associate Professor, AIAA Associate Fellow, araya@mailaps.org
†Doctoral Candidate and Research Assistant, AIAA Student Member
‡Undergraduate Student and Research Assistant
§AIAA Associate Fellow

I. Introduction

High-speed wall-bounded flows play a key role in aerospace applications, such as unmanned supersonic/hypersonic vehicles, scramjets and advanced space aircraft. The development of an extremely thin boundary layer plus the abrupt changes of the wall to freestream flow parameters result in high momentum/thermal gradients with significant impact to the transport phenomena. Hypersonic flows are energetic and result in regions of high temperature, causing internal energy excitation and aerothermodynamics problems Candler.[10] Therefore, the acquired knowledge of the physics behind hypersonic boundary layers can lead to the development of more efficient turbulence modeling or control techniques for aerodynamic heating design, Leyva.[11] Furthermore, most of turbulent boundary layers evolve in space due to turbulent entrainment, showing non-homogeneous conditions along the flow direction. From a computational perspective, spatially-developing turbulent boundary layers (SDTBL) exhibit tremendous challenges due to the need for realistic (having the correct energy power spectra), accurate, and time-dependent inflow turbulence information. The problem becomes harder if one wants to resolve the full energy flow spectrum (i.e., Direct Numerical Simulation or DNS), to evaluate compressibility effects and to account for wall thermal conditions. This article intends to address the nature of the three points previously stated.

Candler[10] in his recent transport phenomena review article in hypersonic flows stated "little effort has been directed toward understanding turbulent motion at the extreme conditions of hypersonic flight." Furthermore, Bertin and Cummings[13] discussed experimental and numerical research efforts done on hypersonic flow and concluded that "there were still many challenges to analyzing and designing high-speed vehicles."

Martin's research group carried out several studies on supersonic-hypersonic flows by means of DNS in order to inspect the effects of wall temperature,[6] Mach number,[7] high enthalpy[8] and initialization[15] on zero-pressure gradient (ZPG) boundary layers, which were performed at low momentum-thickness Reynolds numbers ($Re_{\delta 2} \sim 1600$) or $Re_\tau = \delta u_\tau/\nu_w \sim 500$ in spatial domains with streamwise lengths in the order of 10δ, being δ the inlet boundary layer thickness. In Duan *et al.*,[6] DNS of a flat plate at Mach 5 with the ratio of wall-to-freestream temperature T_w/T_δ from 1.0 to 5.4 was performed, totaling five cases. They found that scaling laws employed in adiabatic compressible boundary layers also hold for non-adiabatic cases. Priebe & Martin[16] studied low-frequency unsteadiness by carrying out DNS over a 24° compression ramp at Mach 2.9 and $Re_\tau = 340$. They utilized the turbulent inflow methodology by Xu & Martin[21] and considered an auxiliary domain ($\sim 8.3\delta$ in length with the recycle plane at 7.3δ) to feed turbulent information to a principal domain ($\sim 14.3\delta$ in length) obtaining a mesh with 28 million points in total. In Araya *et al.*,[3] DNS of turbulent spatially-developing boundary layers was performed over an isothermal flat plate at several flow regimes: incompressible, supersonic (Mach 2.5), and hypersonic (Mach 5). They extended the dynamic turbulent inflow generator for SDTBL proposed by[2] to compressible flows, which avoids the use of empirical functions in the calculation of inlet turbulent scales. More recently, assessment of the Reynolds number dependency was conducted in supersonic SDTBL up to momentum-thickness Reynolds numbers, $Re_{\delta 2}$, in the order of 3000.[4]

Hypersonic turbulent boundary layers at Mach 4.9 with the ratio of wall to recovery temperature from 0.5 to 1.5 were examined via DNS in[22] at $Re_{\delta 2} \approx 1900$ with streamwise domain lengths in the order of 20-boundary layer thicknesses. In terms of Reynolds analogies, they concluded that correlation between the streamwise velocity and temperature fluctuations (i.e., $R_{u'T'}$ and the turbulent Prandtl number, Pr_t, were not affected by wall temperature.

According to,[13] the ultimate goal of CFD would be to perform DNS in hypersonic flow simulation. Furthermore, unsteady predictions of compressible, spatially-developing turbulent boundary layers require not only highly-scalable parallel flow solvers but also significant computational resources. What is more, the need of realiable turbulent inlet conditions and small physical time steps have certainly prevented the advancement of high spatial/temporal resolution numerical simulations or DNS. In the present study, we are considering a dynamic multiscale approach to connect the friction velocities at the inlet and recycle stations, which allows to account for the effects of arbitrary Reynolds and Mach numbers. Thus, there is no need of an empirical correlation as in Lund *et al.*,[14] Urbin & Knight[9] and Stolz & Adams.[17] In DNS, much attention has been paid to the velocity field so far; whereas the temperature field is "in the background." Our focus consists of examining the wall temperature effect on Mach-5 turbulent boundary layers, particularly on local maxima of thermal fluctuations and turbulent heat fluxes, vertical transport of Reynolds shear stresses and momentum/thermal turbulent coherent structures.

II. Turbulent Inflow Conditions and Numerical Details

Unsteady simulations of turbulent spatially-developing boundary layers via DNS is not trivial since high mesh resolution is required in order to resolve the smallest turbulence scales (Kolmogorov and Batchelor scales). Also, the computational box must be large enough to appropriately capture the dynamics of the large-scale turbulent motions. Additionally, it requires the prescription of accurate and realistic turbulent inflow information. In this manuscript, we are employing the inflow generation method proposed by Araya *et al.*,[2] which has been adapted to compressible flow in[4] (inlet instantaneous velocity, temperature and pressure) which is a modified version of the original rescaling-recycling method by Lund *et al.*[14] The basic concept of the rescaling-recycling method is to extract the flow solution (mean and fluctuating components of the velocity, thermal and pressure fields) from a downstream plane (called "recycle") and after performing a transformation by means of scaling functions, the transformed profiles are re-injected at the inlet plane. In Figure 1 can be seen the streamwise locations of the inlet and recycle plane (flow from left to right), the recycle plane being the one located most downstream. In between, the reader can visualize the test plane, whose function is explained later in the present article. Moreover, iso-surfaces of instantaneous density (approximately three-times larger than that of the near wall region) colored by instantaneous streamwise velocity have been plotted. The turbulent boundary layer is divided into inner and outer zones, where different scaling laws are applied[4] in a multiscale fashion. The projection of flow parameters from the recycle plane to the inlet is performed along constant values of y^+ (inner region) and y/δ (outer region). During the re-scaling procedure of the flow parameters, the ratio of the inlet friction velocity to the recycle friction velocity (i.e., $\lambda = u_{\tau,inl}/u_{\tau,rec}$) is required. The friction velocity is defined as $u_\tau = \sqrt{\tau_w/\rho}$, where τ_w is the wall shear stress and ρ is the fluid density. Since the inlet boundary layer thickness must be prescribed according to the desired inlet Reynolds number, prescribing also the inlet friction velocity would be redundant. To solve this issue, Lund *et al.*,[14] Urbin & Knight[9] and Stolz & Adams[17] used the well-known 1/8-power law that connects the friction velocity to the momentum thickness in zero-pressure gradient flows; thus, $u_{\tau,inl}/u_{\tau,rec} = (\delta_{2,inl}/\delta_{2,rec})^{-1/8}$. The empirical power (-1/8) might be strongly affected by external conditions; therefore, we explicitly compute this power, $\gamma_{\delta 2}$, by relating the mean flow solution from a new plane (so-called the "test" plane, as seen in Figure 1) to the solution from the recycle plane as follows:

$$\gamma_{\delta 2} = \frac{ln(u_{\tau,test}/u_{\tau,rec})}{ln(\delta_{2,test}/\delta_{2,rec})}. \tag{1}$$

Figure 2 (a) exhibits time variation of the dynamically computed power law exponent $\gamma_{\delta 2}$ computed by Eq. 1 in the hypersonic flat plate under adiabatic wall condition. It is observed that $\gamma_{\delta 2}$ fluctuates significantly during the transient stage where the time filter was changed in order to quickly remove initial condition effects ("on the fly" mean flow calculation). After approximately 47 flowthroughs, the $\gamma_{\delta 2}$ power tends toward the approximate value of -0.044, which differs in about 65% from the classical empirical value of $-1/8$ for high Reynolds numbers (see White[19]). This confirms the importance of selecting appropriate empirical correlations in numerical simulation, which might be highly impacted by external conditions, for instance the Reynolds number. Moreover, the computed $\gamma_{\delta 2}$ values were -0.076 and -0.059 in the wall cooling and wall heating cases, respectively. This indicates some moderate effect of the wall temperature on the $\gamma_{\delta 2}$ exponent in the hypersonic regime at low Reynolds numbers. Once the exponent $\gamma_{\delta 2}$ is obtained from Eq. 1, the values of $u_{\tau,inl}$ and λ can be calculated. Figure 2 (b) depicts the temporal variation of λ during the simulation of the adiabatic wall condition case, tending toward a value of approximately 1.012.

To perform the proposed DNS, a highly accurate, very efficient, and highly scalable CFD solver is required. The flow solver PHASTA is an open-source, parallel, hierarchic (2^{nd} to 5^{th} order accurate), adaptive, stabilized (finite-element) transient analysis tool for the solution of compressible[20] or incompressible flows (Jansen[12]). PHASTA has been extensively validated in a suite of DNS under different external conditions,[1,5,3,4]

Boundary Conditions: At the wall, the classical no-slip condition is imposed for all velocity components. Cooling, adiabatic and heating wall conditions are assumed for the thermal field with the ratio T_w/T_∞ = 2.25, 5.45 and 8.175, respectively. Here, T_w is the wall temperature and T_∞ is the freestream temperature. The T_r/T_∞ ratios are 0.41, 1 and 1.5, respectively. T_r is the recovery or adiabatic temperature. The lateral boundary conditions are handled via periodicity; whereas, freestream values are prescribed on the top surface.

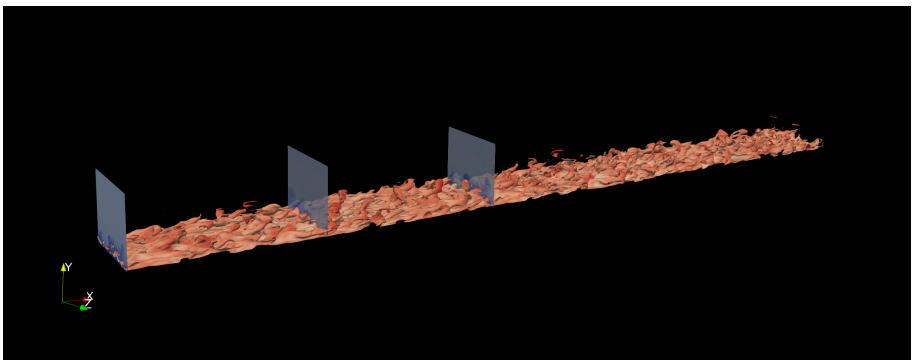

Figure 1. Schematic of the adiabatic hypersonic spatially-developing boundary layer with inlet, recycle and test planes (iso-surfaces of instantaneous density).

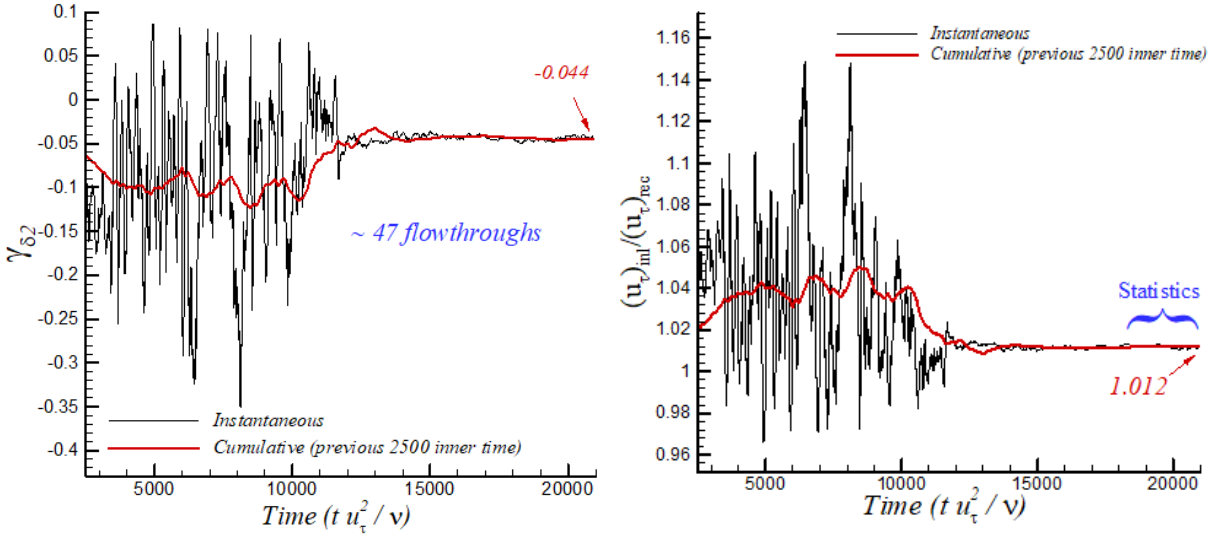

(a) (b)

Figure 2. (a) Time-series of the dynamically computed power-law exponent $\gamma_{\delta 2}$ and (b) friction velocity ratio variation for hypersonic flow and adiabatic wall condition.

Table 1 summarizes the characteristics of hypersonic cases at $M_\infty = 5$ at different wall thermal conditions. Additionally, an incompressible case was considered at similar low Reynolds numbers for compressiblity effect assessment, where temperature was regarded as a passive scalar. Information regarding the Mach number, Reynolds number range, wall thermal condition, computational domain dimensions in terms of the inlet boundary layer thickness δ_{inl} (where L_x, L_y and L_z represent the streamwise, wall-normal and spanwise domain length, respectively) and mesh resolution in wall units (Δx^+, Δy^+_{min}, Δy^+_{max}, Δz^+) is also supplied. In all cases, the number of mesh points in the streamwise, wall-normal and spanwise direction is 440 × 60 × 80, respectively. A similar Von Karman number or shear Reynolds number was prescribed in all cases, i.e., $\delta^+ = 250$. These cases were run in 96 processors in Stampede 2 (TACC) and Comet (SDSC), consuming about 20,000 CPU hours each.

Table 1. Numerical Cases.

Case	M_∞	$Re_{\delta 2}$	Wall Condition	$L_x \times L_y \times L_z$	Δx^+,$\Delta y^+_{min}/\Delta y^+_{max}$, Δz^+
Incomp.	0	306-578	Isothermal	$45\delta_{inl} \times 3.5\delta_{inl} \times 4.3\delta_{inl}$	14.7, 0.2/13, 8
Hyp. 1	5	363-659	T_w/T_∞=2.25, T_w/T_r=0.41	$44\delta_{inl} \times 3.5\delta_{inl} \times 4.3\delta_{inl}$	13.3, 0.17/16.7, 7.4
Hyp. 2	5	600-1014	T_w/T_∞=5.45, T_w/T_r=1	$43\delta_{inl} \times 3.5\delta_{inl} \times 4.3\delta_{inl}$	16, 0.21/20, 9
Hyp. 3	5	752-1248	T_w/T_∞=8.175, T_w/T_r=1.5	$43\delta_{inl} \times 3.5\delta_{inl} \times 4.3\delta_{inl}$	17, 0.21/20, 9

III. DNS Results

For the time-averaged streamwise velocity in wall units and compressible flow, the Van Driest transform is applied,

$$U_{VD} = \int_0^U \left(\frac{T_w}{T}\right)^{1/2} dU \tag{2}$$

Figure 3 (a) depicts the mean streamwise velocity normalized by the freestream velocity. The adiabatic case (Hyp. 2) agrees very well with DNS data from Duan *et al.*[6] at similar Reynolds numbers. In addition, validation of present adiabatic DNS case was performed by a comparison with experiments by Tichenor[18] at significantly higher Reynolds numbers. Notice the good agreement in the outer region. Furthermore, significant increase of U are observed in the log region as the Mach number increases (up to 10%). For the hypersonic regime, local flow acceleration is detected as the wall temperature increases; whereas a reduction of the mean streamwise velocity is obtained under wall cooling influence. In fact, this flow retardation is clearly observed in fig. 3 (b).
Turning to the mean static temperature in supersonic flow, the T/T_∞ and U/U_∞ relationship is expressed in terms of the Walz's equation,

$$\frac{T}{T_\infty} = \frac{T_w}{T_\infty} + \frac{T_r - T_w}{T_\infty}\left(\frac{U}{U_\infty}\right) - r\frac{\gamma - 1}{2}M_\infty^2\left(\frac{U}{U_\infty}\right)^2 \tag{3}$$

where r is the recovery factor ($= Pr^{1/3}$) and T_r the well known recovery temperature. Figure 3 (c) shows the mean static temperature vs. mean streamwise velocity both normalized by the corresponding freestream value. Overall, the Walz equation gives excellent predictions for the adiabatic and wall heating cases in hypersonic flows. On the other hand, some overprediction was observed in wall cooling (up to 7%). This is consistent with DNS results by Duan *et al.*[6] (see ⋄ symbol in fig. 3 (c)).
Figure 4 illustrates the streamwise variation of local maxima of fluctuations in cases from Table 1. Major conclusions can be described as follows: (i) hypersonic cases show larger maxima of u'_{rms} with respect to the incompressible regime, (ii) $(u'_{rms})_{max}$ increases as the wall temperature increases in hypersonic flow, (iii) variation in peaks of $< u'v' >$ are within 15%, and (iv) the largest normalized values for the thermal fluctuations t'_{rms} and vertical heat fluxes $< v't' >$ were found for the wall cooling case, with increases of up to 7% with respect to the adiabatic case.

Figure 5 (a) depicts the wall-normal transport of Reynolds shear stresses or triple correlation $< v'u'v' >$ in outer units. It is observed that transport of Reynolds shear stresses significantly increases as the wall temperature increases in the hypersonic regime. It is worth noting that wall cooling induces a change in the

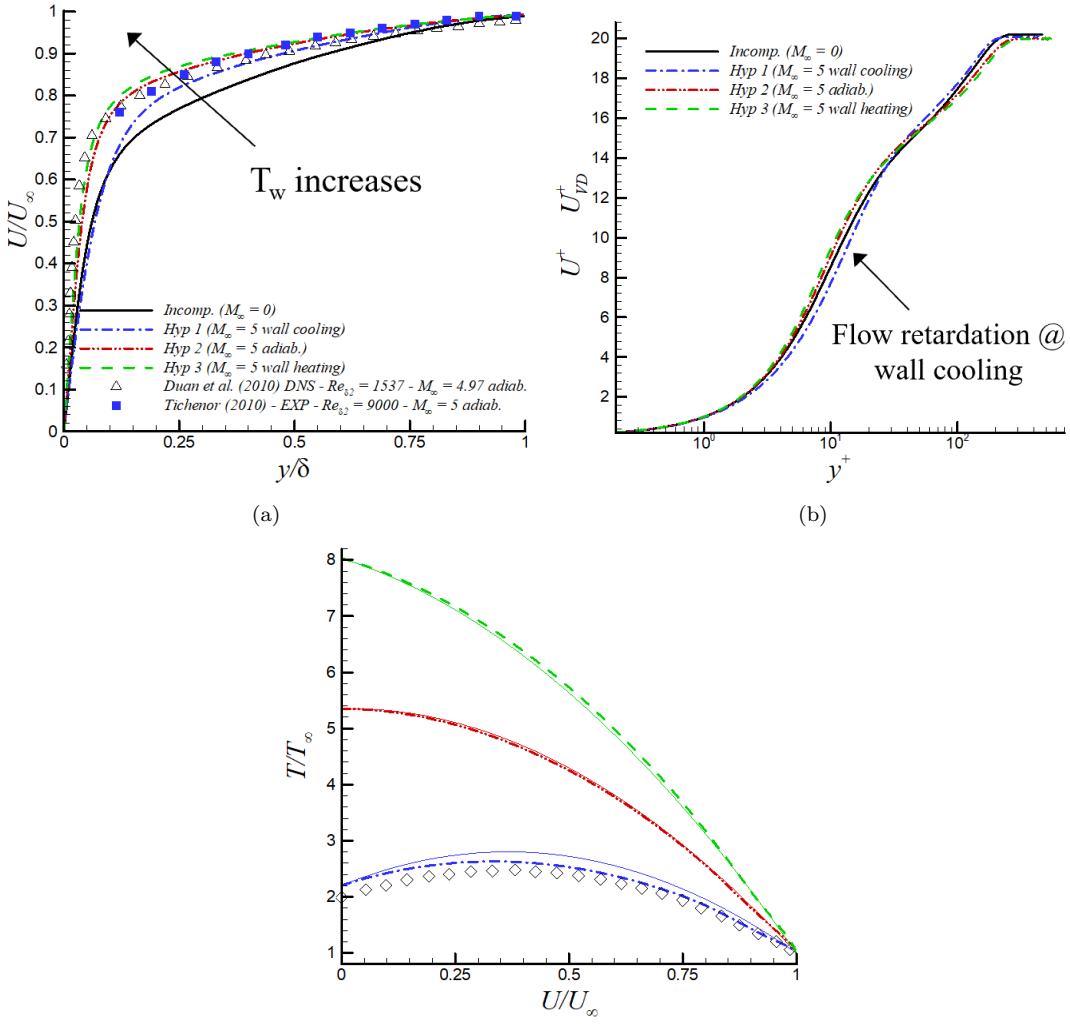

(a) (b)

(c)

Figure 3. Mean streamwise velocity in (a) outer units, (b) inner units, and (c) mean static temperature.

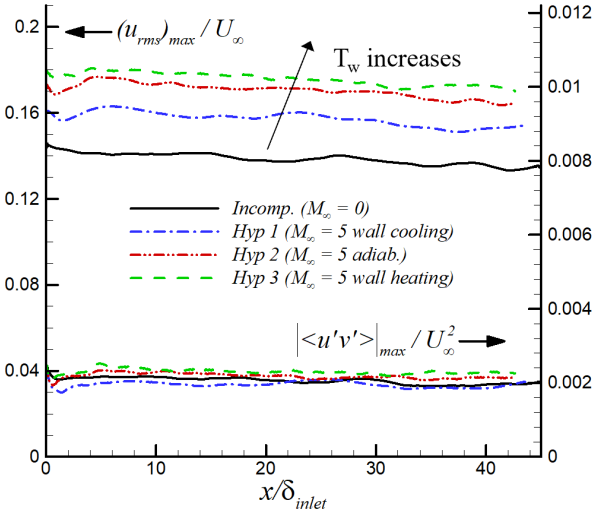

(a)

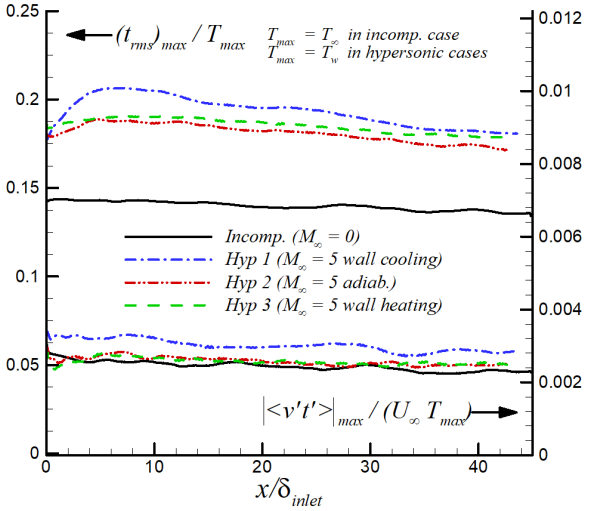

(b)

Figure 4. Streamwise variation of local maxima: (a) u_{rms} and $< u'v' >$, (b) t_{rms} and $< v't' >$

transport direction in the near-wall region, caused by local overheating of the boundary layer. It was found that this overheating enhances ejection or Q2 events, as seen in fig. 5 (b) at $y/\delta \approx 0.01$.

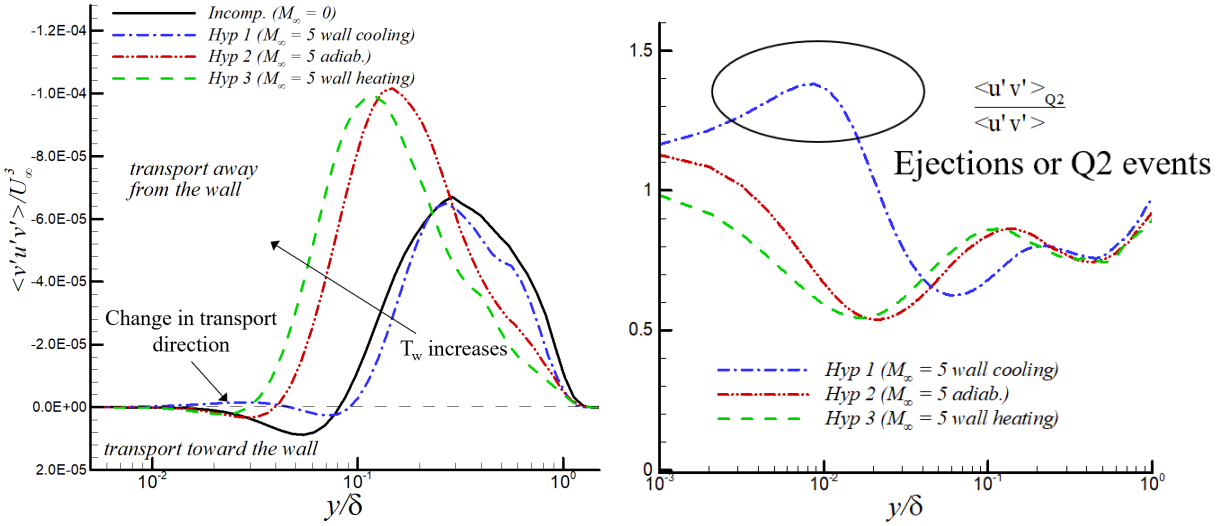

(a) (b)

Figure 5. (a) Vertical transport of $< u'v' >$ and (b) Q2 contributions to $< u'v' >$ in outer units.

A. Wall Temperature Assessment on Coherent Structures

In Figure 6, flow visualization of thermal large-scale motions has been carried out by extracting iso-surfaces of normalized instantaneous temperature in hypersonic flows, i.e., $(T - T_w)/(T_\infty - T_w) = 0.75$. It can be concluded that large thermal turbulent structures are more organized but more anisotropic with more intense "gaps" of freestream fluids in between when wall cooling is applied, as seen in fig. 6 (a) (similar to incompressible thermal coherent structures, not shown here). On the other hand, the thermal structures become less organized (but more isotropic) as the wall temperature is increased. Particularly, a much "finer" structure of thermal coherent motions is observed in the wall heating case (6 (c)) in comparison with the rest (wall cooling and adiabatic). Figures 7 and 8 depict iso-surfaces of two-point correlation (TPC) of streamwise velocity and thermal fluctuations, respectively, at $y^+ = 15$ (left) and 50 (right) for the different hypersonic cases. Images on the top correspond to the wall cooling case, images on the middle describe adiabatic wall condition, and finally, images on the bottom correspond to the wall heating case. The value of $y^+ = 15$ corresponds to the location of peak values of the u'_{rms} in the buffer layer, while $y^+ = 50$ approximately coincides with the log region in the outer part of the boundary layer. Positive red iso-surfaces were extracted at a value of 0.125 of the normalized TPC, whereas a value of -0.125 was considered in the extraction of negative blue iso-surfaces. Generally speaking, the major turbulent structure (in red) are flanked by two secondary turbulent structures (blue).

In terms of TPCs of u' in Figure 7, there is a significant enlargement of the major turbulent structure for the same wall thermal condition as one moves further from the wall. Also, the flow exhibits an important level of correlation upstream of the reference plane in the outer region of the boundary layer. Similar trends were observed in the negatively correlated "flanking" structures. It is worth noting the presence of extremely long turbulent structures in the buffer zone of hypersonic boundary layers subject to wall thermal cooling, expanding roughly 4.5δ in the streamwise direction, as seen in fig. 7 (a). At the same y^+ location, the influence of increasing the wall temperature can be described as a shortening process of the turbulent structures. This is consistent with previous conclusions of ejection event enhancement (or Q2 events) under wall cooling condition. Ejections would pump up low speed fluid, contributing to the formation of low speed streaks.

Turning to thermal turbulent coherent structures, TPCs of t' in figure 8 exhibit some differences with TPCs of u' in hypersonic flat plates subject to various wall temperature conditions. For instance, the streamwise lengths of positive iso-surfaces of R_{tt} are much smaller than those of R_{uu}, about 50% shorter in length. In addition, the flanking negative thermal structures look much tinier than in the velocity field, and nearly

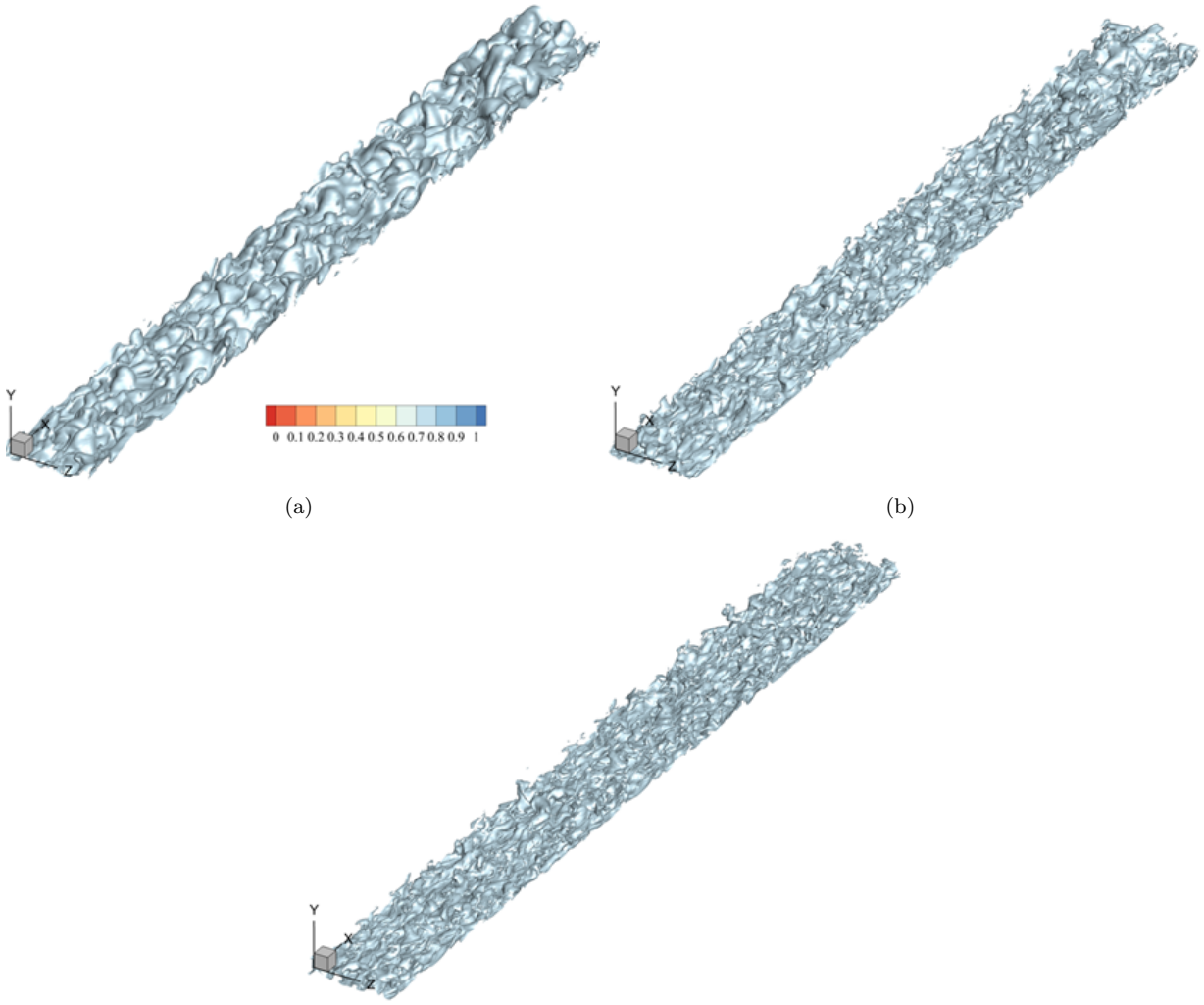

Figure 6. Visualization of thermal large-scale motions: iso-surfaces of normalized instantaneous temperature in hypersonic flows. (a) wall cooling, (b) adiabatic and (c) wall heating.

disappear in the outer region.

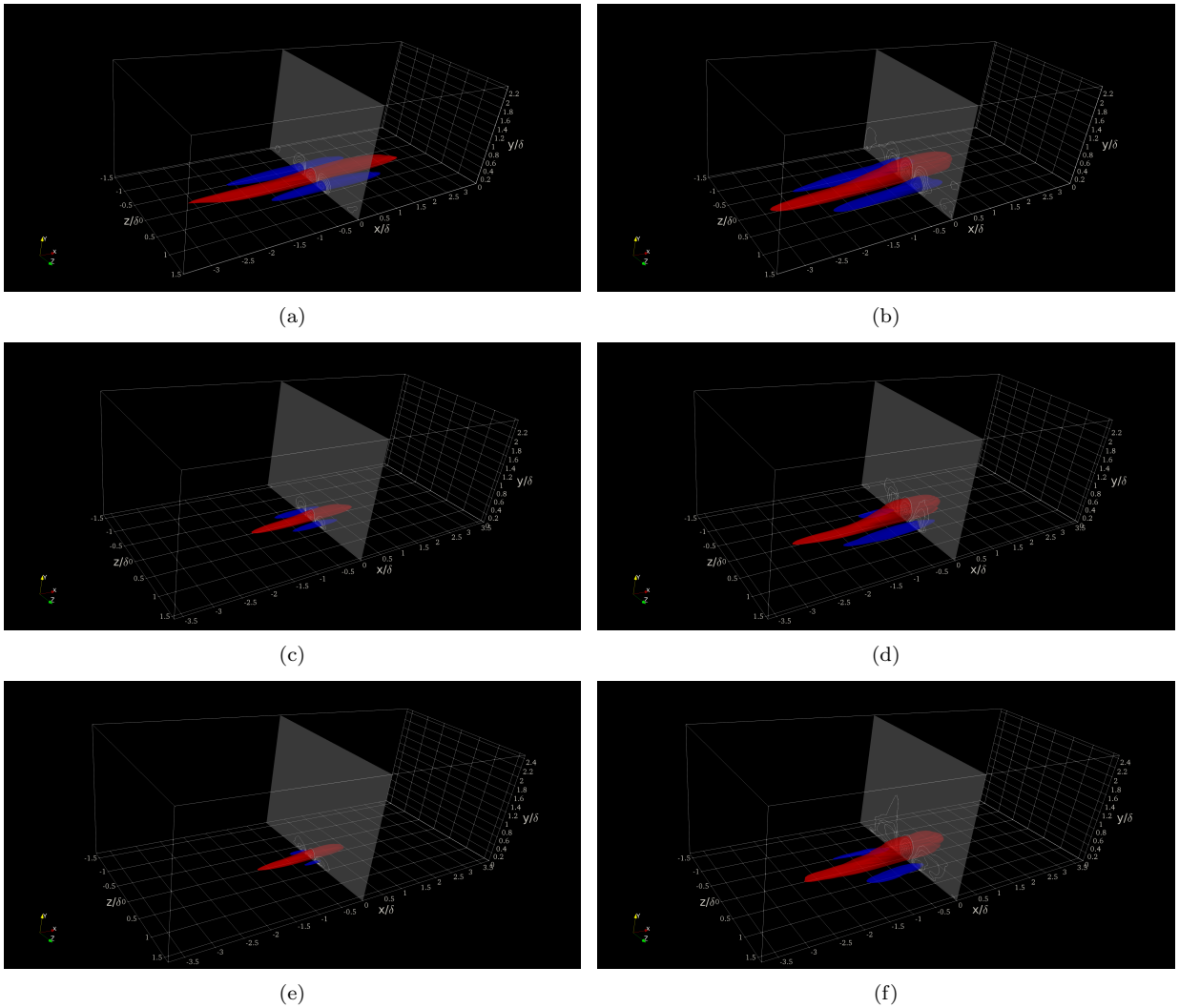

(a) (b) (c) (d) (e) (f)

Figure 7. Wall temperature effect on momentum turbulent structures: (a) wall cooling $y^+ = 15$, (b) wall cooling $y^+ = 50$, (c) adiabatic $y^+ = 15$, (d) adiabatic $y^+ = 50$, (d) wall heating $y^+ = 15$, and wall heating $y^+ = 50$.

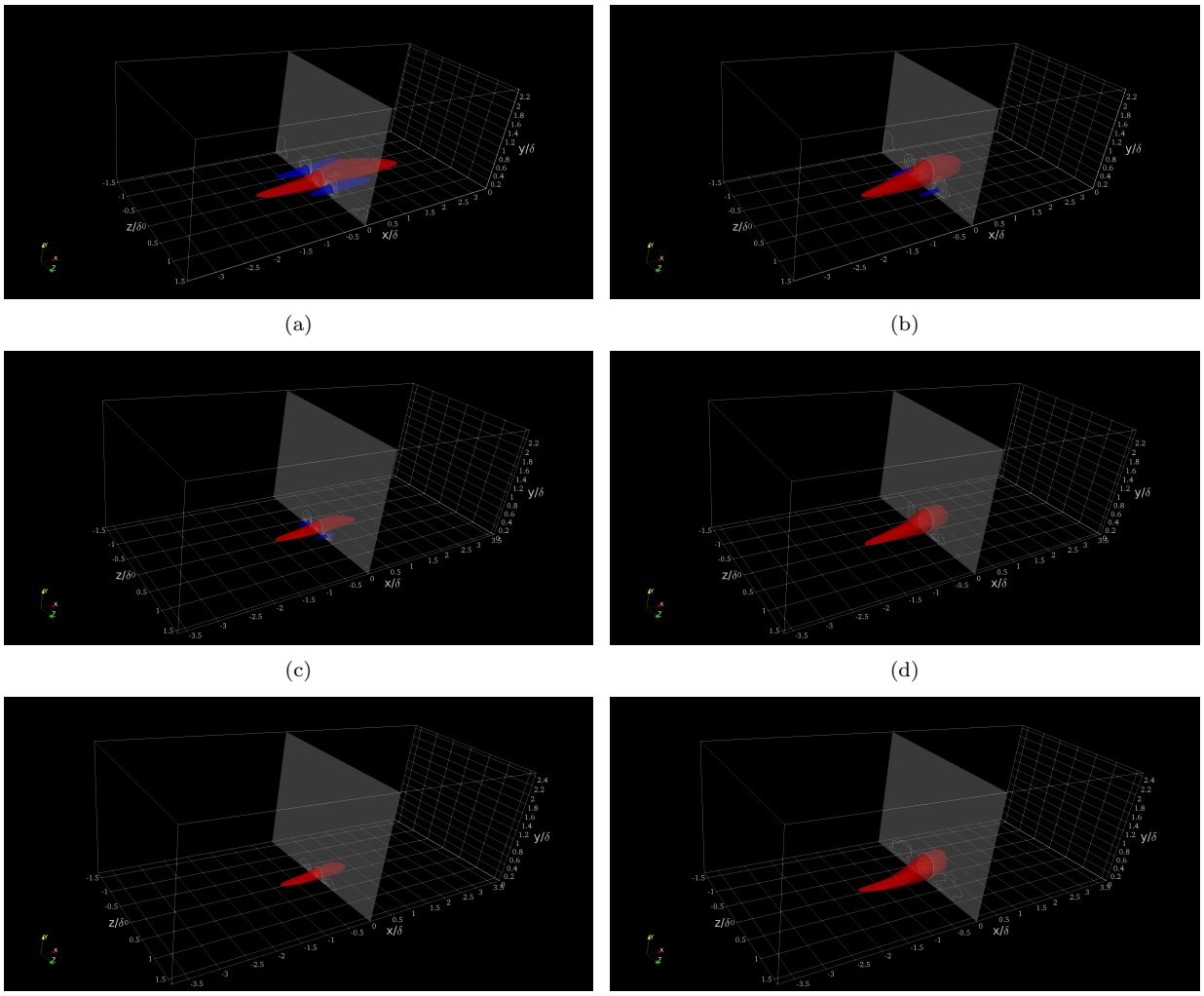

(a) (b) (c) (d) (e) (f)

Figure 8. Wall temperature effect on thermal turbulent structures: (a) wall cooling $y^+ = 15$, (b) wall cooling $y^+ = 50$, (c) adiabatic $y^+ = 15$, (d) adiabatic $y^+ = 50$, (d) wall heating $y^+ = 15$, and wall heating $y^+ = 50$.

B. Joint Probability Density Function

A probability distribution analysis of quadrant events has been performed in Reynolds shear stresses $< u'v' >$ at $y^+ = 5$ and 50 for the four cases studied, as seen in figs. 9 and 10, respectively. A significant enhancement of ejection events (Q2) and inward interactions (Q3) is observed in wall cooling, caused by the local overheating in the near wall region of the boundary layer. The rotated "ellipsoid" distributions of u' and v' are very similar in the incompressible flow regime as compared with the adiabatic and wall heating hypersonic cases in the viscous sublayer. Similar trends of JPDF for low probability values (i.e., 0.06) are observed in the log region in all cases. However, the high probability density zone at 0.18 looks more concentrated in the fourth quadrant (sweep events) for the wall cooling case.

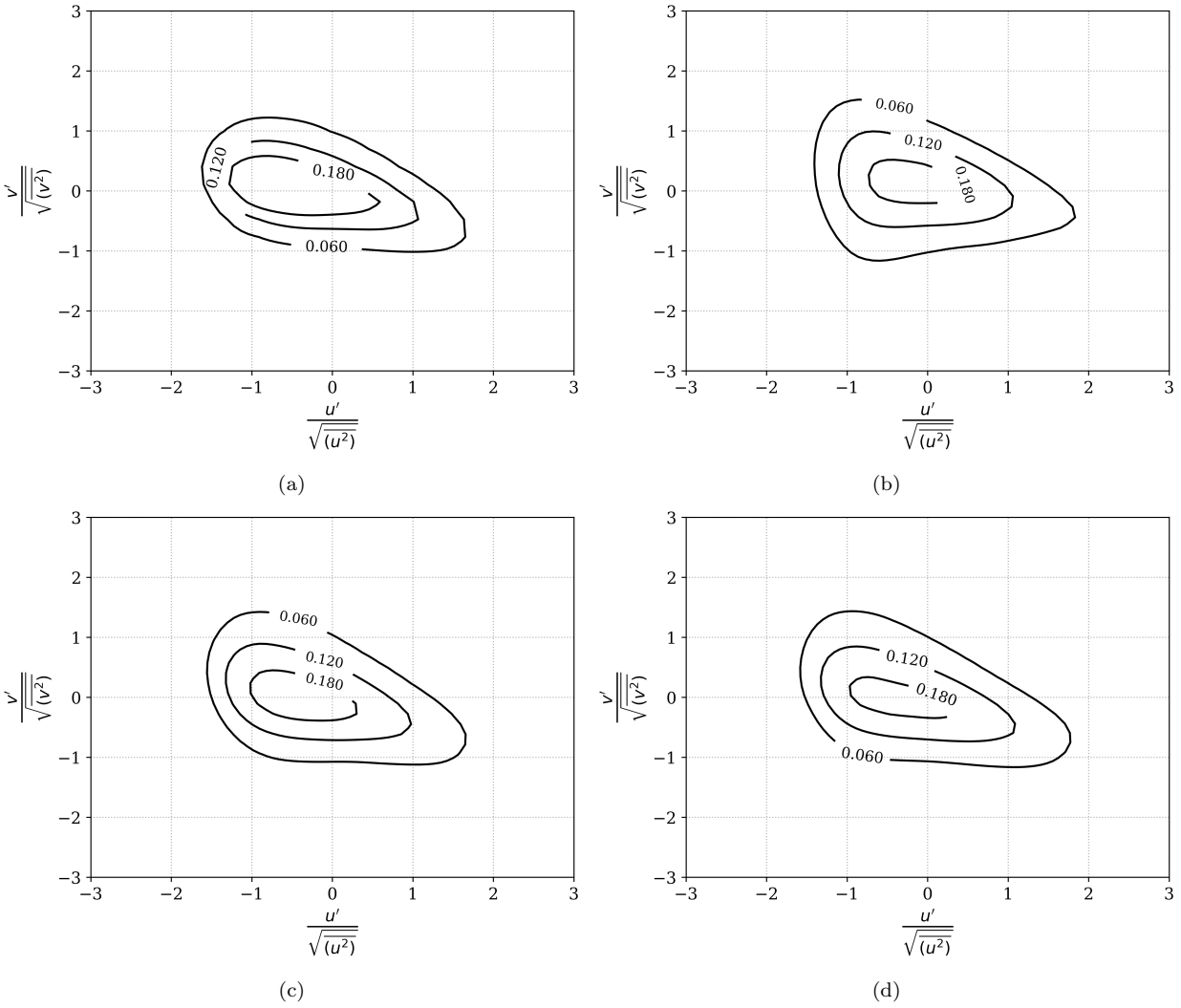

Figure 9. JPDF of Reynolds shear stresses $< u'v' >$ at $y^+ = 5$: (a) incompressible, (b) wall cooling, (c) adiabatic, and (d) wall heating.

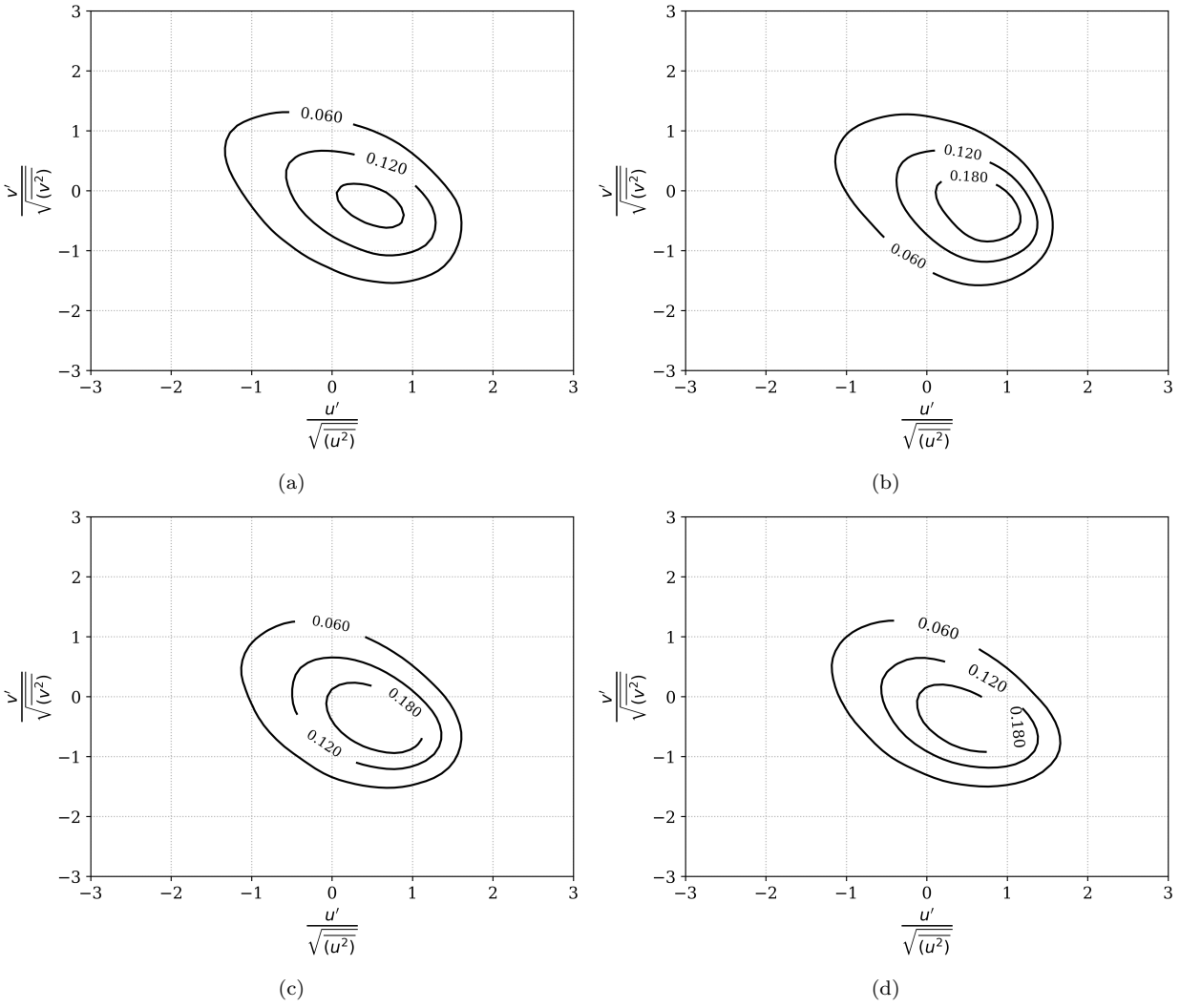

Figure 10. JPDF of Reynolds shear stresses $< u'v' >$ at $y^+ = 50$: (a) incompressible, (b) wall cooling, (c) adiabatic, and (d) wall heating.

IV. Conclusions

Direct simulation of hypersonic turbulent boundary layers over a flat plate is carried out at various wall temperature conditions and low Reynolds numbers. It was observed that vertical transport of Reynolds shear stresses significantly increase as the wall temperature increases in the hypersonic regime. Interestingly, wall cooling induced a transport direction change in the near wall region due to the local overheating of the boundary layer, which in turn caused intensification of ejections. Along the same lines, this ejection enhancement seemed to be the reason of the extremely long structures found in the buffer zone of hypersonic boundary layer subject to wall cooling. Furthermore, large thermal turbulent structures are more organized (anisotropic) with more intense "gaps" of freestream fluids in between when wall cooling is applied. The thermal structures become less organized but more isotropic as the wall temperature is increased.

V. Acknowledgment

This material is based upon work supported by the Air Force Office of Scientific Research under award number FA9550-17-1-0051. GA acknowledges NSF Grant #1847241. Computational resources are supplied by XSEDE project #TG-CTS170006 and a Broadening Participation Allocation at Blue Waters.

References

[1]G. Araya, C. Castillo, and F. Hussain. The log behaviour of the Reynolds shear stress in accelerating turbulent boundary layers. *Journal of Fluid Mechanics*, 775:189–200, 2015.

[2]G. Araya, L. Castillo, C. Meneveau, and K. Jansen. A dynamic multi-scale approach for turbulent inflow boundary conditions in spatially evolving flows. *Journal of Fluid Mechanics*, 670:518–605, 2011.

[3]G. Araya, C. Lagares, and K.E. Jansen. Direct simulation of a Mach-5 turbulent spatially-developing boundary layer. *49^{th} AIAA Fluid Dynamics Conference, AIAA AVIATION Forum, (AIAA 3131876) 17 - 21 June, Dallas, TX*, 2019.

[4]G. Araya, C. Lagares, and K.E. Jansen. Reynolds number dependency in supersonic spatially-developing turbulent boundary layers. *2020 AIAA SciTech Forum (AIAA 3247313) 6 - 10 January, Orlando, FL.*, 2020.

[5]A. Doosttalab, G. Araya, J. Newman, R. Adrian, K. Jansen, and L. Castillo. Effect of small roughness elements on thermal statistics of a turbulent boundary layer at moderate Reynolds number. *Journal of Fluid Mechanics*, 787:84–115, 2015.

[6]Duan, L. and Beekman, I. and Martin, M. P. Direct numerical simulation of hypersonic turbulent boundary layers. part 2. effect of wall temperature. *Journal of Fluid Mechanics*, 655:419–445, 2010.

[7]Duan, L. and Beekman, I. and Martin, M. P. Direct numerical simulation of hypersonic turbulent boundary layers. part 3. effect of mach number. *Journal of Fluid Mechanics*, 672:245–267, 2011.

[8]Duan, L. and Martin, M. P. Direct numerical simulation of hypersonic turbulent boundary layers. part 4. effect of high enthalpy. *Journal of Fluid Mechanics*, 684:25–59, 2011.

[9]G. Urbin and D. Knight. Large-Eddy Simulation of a supersonic boundary layer using an unstructured grid. *AIAA Journal*, 39(7):1288–1295, 2001.

[10]Graham V. Candler. Rate effects in hypersonic flows. *Annual Review of Fluid Mechanics*, 51:379–402, 2019.

[11]Ivett A. Leyva. The relentless pursuit of hypersonic flight. *Physics Today*, 70, 11, 30, doi: 10.1063/PT.3.3762, 2017.

[12]K. E. Jansen. A stabilized finite element method for computing turbulence. *Comp. Meth. Appl. Mech. Engng.*, 174:299–317, 1999.

[13]John J. Bertin and Russell M. Cummings. Critical hypersonic aerothermodynamic phenomena. *Annual Review of Fluid Mechanics*, 38:129–157, 2006.

[14]T.S. Lund, X. Wu, and K.D. Squires. Generation of turbulent inflow data for spatially-developing boundary layer simulations. *Journal of Computational Physics*, 140(2):233–258, 1998.

[15]Martin, M. P. Direct numerical simulation of hypersonic turbulent boundary layers. part 1. initialization and comparison with experiments. *Journal of Fluid Mechanics*, 570:347–364, 2007.

[16]Priebe, S. and Martin, M. P. Low-frequency unsteadiness in shock wave-turbulent boundary layer interaction. *Journal of Fluid Mechanics*, 699:1–49, 2012.

[17]S. Stolz and N. Adams. Large-eddy simulation of high-Reynolds-number supersonic boundary layers using the approximate deconvolution model and a rescaling and recycling technique. *Physics of Fluids*, 15(8):2398–2412, 2003.

[18]N. T. Tichenor. Characterization of the influence of a favorable pressure gradient on the basic structure of a Mach 5.0 high Reynolds number supersonic turbulent boundary layer. *Ph.D. dissertation, Texas A and M University*, 2010.

[19]F. M. White. *Viscous Fluid Flow.* McGraw-Hill Mechanical Engineering, New York, 2006.

[20]C. H. Whiting, K. E. Jansen, and S. Dey. Hierarchical basis in stabilized finite element methods for compressible flows. *Comp. Meth. Appl. Mech. Engng.*, 192(47-48):5167–5185, 2003.

[21]S. Xu and M. P. Martin. Assessment of inflow boundary conditions for compressible turbulent boundary layers. *Physics of Fluids*, 16(7):2623–2639, 2004.

[22]You-Biao Chu, Yue-Qing Zhuang and Xi-Yun Lu. Effect of wall temperature on hypersonic turbulent boundary layer. *Journal of Turbulence*, 14(12):37–57, 2013.